Simulations of breakthrough curves for fixed-bed column adsorption of cobalt (II) ions on spent tealeaves

Kibrewossen Tesfagiorgis, Abel E. Navarro, Bow Ming Chen, Nicholas Herrera, Joel Hernandez, Álvaro González-Álvarez and Ousmane Sy Savane

ABSTRACT

The objective of this study is to model the breakthrough adsorption curves of Co (II) ions using spent tealeaves in fixed-bed column experiments. Spent leaves of green tea (GT), peppermint tea (PM) and chamomile (CM) were packed in glass columns with a diameter of 2 cm and height of 15 cm, and used as filters for the removal of the pollutant. Aqueous solutions of cobalt (II) ions (100 mg/L) at pH 6 were prepared and pumped against gravity through the columns at a uniform flow rate of 5 mL/min. Breakthrough curves were fitted for the residual concentration data using the Thomas, Yoon-Nelson, and Clark models, with added empirical terms to delineate the lower tail of the breakthrough curve. These mathematical models were successfully linearized using the natural logarithm for parameter estimation. The results reveal that the Co (II) adsorption fits all three models for all the adsorbents. The Thomas model indicated that the calculated adsorption capacities followed the trend: PM > GT > CM with values of 59.7, 25.2, and 24.9 mg/g respectively. Moreover, CM showed the highest adsorption rates with all the mathematical models, whereas Yoon-Nelson theory provided evidence that PM has the longest 50% adsorption breakthrough among the adsorbents. Lastly, morphological and textural studies indicate that all spent leaves are good candidates as adsorbents due to their high surface heterogeneity. This study proposes the use of spent tealeaves as Co (II) adsorbents because they are inexpensive and environmentally beneficial.

Key words | adsorption, breakthrough curve, fixed-bed, heavy metal, modeling

Kibrewossen Tesfagiorgis (corresponding author)
Abel E. Navarro
Bow Ming Chen
Nicholas Herrera
Joel Hernandez
Science Department,
Borough of Manhattan Community College,
City University of New York, NY 10007,
USA
E-mail: *ktesfagiorgis@bmcc.cuny.edu*

Álvaro González-Álvarez
Boswell Engineering,
South Hackensack, NJ 07606,
USA

Ousmane Sy Savane
Bureau of Water Supply (BWS),
Distribution Water Quality Operation (DWQO),
New York City Environmental Protection,
New York,
USA

HIGHLIGHTS

- Simulation of fixed-bed column adsorption of heavy metals on spent tealeaves.
- Added empirical terms to the most popular kinetic fixed-bed models to simulate the lower tails of the breakthrough curve.
- A meaningful correlation between structural features and adsorption of pollutants has been made using SEM analysis.
- Sensitivity analysis of the model parameters were done by varying the parameters around optimal values.

INTRODUCTION

The objective of this study is to model the breakthrough curve for fixed-bed adsorption column experiments using spent tealeaves as potential adsorbent of Co (II) from contaminated solutions. The scientific community has always been concerned about the prevalence of heavy metals in industrial wastewater and surface waters in general (Sotelo *et al.* 2013; Patel 2019). The current techniques for the purification of water are not highly selective and cannot be

doi: 10.2166/wst.2020.295

applied under different experimental conditions. Removal of pollutants using different materials as biomass has been evaluated (Massimi *et al.* 2018), among which spent tealeaves in a fixed-bed column has become popular in bioremediation due to the following important attributes of the methodology: inexpensive, eco-friendly, no sludge generation, and adsorbent recovery. Spent tealeaves mainly contain cellulose (the most abundant polysaccharide on the planet) and have organic functional groups such as carboxyl, amino, and hydroxyl. The presence of these functional groups in spent tealeaves has been confirmed by infrared spectroscopy (Jung *et al.* 2014). Due to their high polarity, these groups are active adsorption sites for cations (heavy metal ions) and polar pollutants (i.e. phenols). Furthermore thermogravimetric analyses of chai tea as an adsorbent of Cu (II) indicate that spent tealeaves resist temperatures as high as 230 °C without substantial mass loss (Kim *et al.* 2013). This thermal resistance has been associated with the mechanical and physical properties of these biomaterials as suitable adsorbents.

Ahluwalia & Goyal (2005) used tealeaves to remove lead, iron, zinc and nickel ions from contaminated solutions, reporting removal rates of 96, 91, 72, and 58 %, respectively. Mahvi *et al.* (2005) found that tealeaves removed lead at a higher rate than cadmium and nickel from industrial wastewaters. Rengaraj & Moon (2002) investigated the kinetics involved in the removal of Co (II) in wastewater, indicating that more than 90% of the adsorption took place within the first 15–20 min of contact time. Zuorro & Lavecchia (2010) achieved adsorption rates of 98% to 99% for Pb^{2+} in wastewater on black and green spent tealeaves. Yang & Cui (2013) applied alkali-treated tea residue, which resulted in a higher porous surface structure than tealeaves without the treatment, which led to higher removal rates of Pb^{2+}. Malakahmad *et al.* (2016) evaluated the cost-effectiveness of black tealeaves for removal of Ni^{2+} and Zn^{2+} ions from aqueous solution under optimized conditions of pH, contact time, and adsorbent dose.

In this investigation, raw spent tealeaves were packed in glass columns and used as adsorption bio-filters for the adsorption of Co^{2+} metal ions from contaminated solutions. The performance and efficiency of each filter can be mathematically described through the concept of the breakthrough curve defined as a plot of relative pollutant concentration versus time. The breakthrough curve and the time for breakthrough appearance provides crucial characteristics for determining the operation and the dynamic response of a column in addition to: (a) providing a mathematical simulation of the column experiment; (b) explaining the column adsorption process; and (c) outlining the importance of the time for breakthrough and the shape of the curve for determining the operation at medium and large scales and the dynamic response of an adsorption column. Kinetic models are linearized from their original non-linear equations and fitted to mathematical models to describe the behavior of the column. The linearization approach to the mathematical modeling is both easier to use and interpret. The process of linearization is important for parameter estimation.

MATERIALS AND METHODS

Adsorbent preparation and column experiments

Green tea, peppermint tea, and chamomile bags were purchased at a local market. Then, they were taken to the laboratory to be washed, boiled in distilled water, and finally oven-dried. These spent tea samples were used without further mechanical or chemical modification in the physical adsorption tests. Dried samples were packed in Pyrex glass columns with diameters and heights of 2 cm and 15 cm, respectively. Aqueous solutions of cobalt (II) ions (100 mg/L) were prepared and pumped against gravity through the columns at a uniform flow rate of 5 mL/min at pH 6. Samples of the column effluent were collected every minute using a fraction collector. The residual concentrations of the samples were measured using spectroscopy at 600 nm, using the zincon method, which produced a colored solution.

Breakthrough models

Once the effluent samples were collected, breakthrough curves were derived using the mathematical models of Thomas, Clark, and Yoon-Nelson. These models were chosen because of their widespread application in this type of adsorbent/adsorbate system. Linearization was needed to determine the models' parameters. Matrix Laboratory (MATLAB-Version R2019b, MathWorks, Inc., Natick, MA, USA) codes were created for the overall investigation of the breakthrough curve. The MATLAB program was broken into three parts: (a) the linearization of the experimental data to determine the models' parameters; (b) the mathematical simulation and fitting of the raw data; and (c) analysis of parameter sensitivity.

Clark model

$$\frac{C_t}{C_0} = \left(\frac{1}{1 + Ae^{-rt}}\right)^{\frac{1}{n-1}} \quad (1)$$

The Clark model is a relatively new simulation of the breakthrough curves and is based on the use of the mass-transfer concept in combination with the Freundlich isotherm as well as the flow, which is assumed to be piston type. The model has been used in the adsorption of Co (II) with adsorbents *tectona grandis*, (Vilvanathan & Shanthakumar (2017a, 2017b)). Equation (1) is the generalized logistic function for the Clark function. A (min) is the Clark's model parameter which correlates to the breakthrough time, and the breakthrough concentration. The parameter n is the Freundlich isotherm constant, and $1/n$ also represents the isotherm between the adsorbent and solvent; the parameter r (mg $L^{-1} \times min^{-1}$) correlates the mass transfer coefficient (h^{-1}), the flow rate of the solvent per unit of the cross-sectional area, and the velocity of the adsorption zone. These constants were determined by the linearization of the model and plotting C_t/C_0 versus time (t) at the specific bed height (15 cm) and flow rate (5 mL/min).

Thomas model

$$\frac{C_t}{C_0} = \frac{1}{1 + exp\left[\left(\frac{k_{TH}q_e x}{Q}\right) - k_{TH}C_0 t\right]} \quad (2)$$

The model was used effectively to adsorb Co (II) on carboxylated sugarcane bagasse (Xavier *et al.* 2018). Equation (2) represents the Thomas model based on the assumption of Langmuir kinetics of adsorption-desorption without axial dispersion. k_{TH} is the Thomas rate constant that represents the kinetic coefficient (mL $min^{-1} \times mg^{-1}$), q_e (mg/g) is the adsorption capacity, x is the mass of the adsorbent (g), and Q is the influent flow rate (mL/min). The variables x and Q are obtained during the experiment. We used 2.001 g, 3.32 g, and 2.796 g of masses for CM, GT and PM respectively. Q was set up to be 5 mL/min throughout the study while the other parameters were determined from the linearization of the model. According to preliminary data, adsorption kinetics of Co (II) onto GT, CM and PM follow pseudo-second order models with high correlation coefficients (unpublished results). The Thomas model is derived with the assumption that the rate driving force obeys second-order reversible reaction kinetics.

Yoon-Nelson model

$$\frac{C_t}{C_0 - C_t} = \exp(k_{yn}t - \tau k_{yn}) \quad (3)$$

The Yoon-Nelson equation is displayed in Equation (3). This model ignores adsorbate details and the physical properties of the adsorption bed, as shown in Equation (3) (Saadi *et al.* 2013). Therefore, the Yoon-Nelson model is the least complicated theoretical model for describing column performance. It has been fitted to the dynamic adsorption of Co (II) on to aqueous solution using *Chrysanthemum indicum* (Vilvanathan & Shanthakumar (2017a, 2017b). According to Equation (3), k_{yn} is the rate constant (min^{-1}) and τ (min) is the time required for 50% adsorbate breakthrough. The values of k_{yn} and τ were determined from the slope and intercept of the linear plot of $\ln[C_t/(C_0 - C_t)]$ and t.

Parameter estimation

The Freundlich isotherm constant, n in the Clark model, were determined experimentally as 2.18, 2.07 and 1.98 for CM, GT and PM respectively. The model parameters except n were determined by linearizing the mathematical equations. Since the breakthrough functions involve exponentials, and the natural logarithm function was used to linearize them as follows:

The linearized form of Clark model

$$\ln\left[\left(\frac{C_0}{C_t}\right)^{n-1} - 1\right] = -rt + \ln A \quad (4)$$

The linearized form of the Thomas model

$$\ln\left(\frac{C_0}{C_t} - 1\right) = \frac{k_{TH}q_e x}{Q} - k_{TH}C_0 t \quad (5)$$

The linearized form of the Yoon-Nelson model

$$\ln\left(\frac{C_t}{C_0 - C_t}\right) = k_{yn}t - \tau k_{yn} \quad (6)$$

First degree Polyfit MATLAB function was used to determine the model parameters.

Morphological and textural analyses of the adsorbents

Scanning electron microscopy (SEM) analyzed the surface of the three adsorbents using a Table Top Microscope TM3000 (Hitachi). Samples were directly observed in the microscope without any conductive gold film. The microscope has a resolution of 40 nm, which allows us to identify the roughness, texture and morphology of the surfaces. An ideal adsorbent displays pores, pockets, valleys and protrusions where the pollutant is trapped or housed.

RESULTS

The adsorption model functions of Clark, Thomas and Yoon-Nelson were linearized by converting them to logarithmic functions. All linear forms of the functions are shown in Equations (4)–(6). Experimental data were fitted to all these models and the summary of the calculated parameters is displayed in Table 1. In the Clark's linearized model, the parameters – r and ln (A) represent the slope and y-intercept of the time versus $ln((C_0/C_t)^{n-1} - 1)$ graph. The calculated values for the Clark's adsorption rate constant for CM, GT and PM were 0.109, 0.06 and 0.036 mg L^{-1} min^{-1}, respectively. Similar results were recently published by Patel (2019), where the best adsorbents showed lower adsorption rates. Patel (2019) also predicted that an increase in the influent flow rate would also increase the adsorption rate (r). Similarly, the values of the parameter A were determined as the exponents of the y-intercept of the linearized graph (Figure 1 and Table 1). The values of parameter A for the Clark model are 38.2, 27.1, and 54.8 for CM, GT and PM, respectively.

In the linearized Thomas model, $-k_{TH}C_0$ and $k_{TH}{}^*q_{ex}/Q$ represent the slope and y-intercept, respectively. Since the value of C_0 is known, k_{TH} is determined from the slope of the graph (Figure 2). The optimal values of k_{TH} are 0.351, 0.191 and 0.116 for CM, GT and PM respectively. PM had the smallest k_{TH} value, indicating that PM exhibits a maximum contaminant uptake per unit flow. Once k_{TH} values are determined, the adsorption capacity, q_e, values were determined from the y-intercept as: $q_e = Q^*y\text{-intercept}/(k_{TH}{}^*q_{ex})$. CM, GT, and PM samples showed calculated equilibrium adsorption capacities of 24.85, 25.2 and 59.7 (mg/g), respectively. These results corroborate the Clark's model, which also indicated that PM is a better adsorbent than CM and GT. Other adsorbents were also used in the removal of Co (II) ions in column adsorption with similar results. Vijayaraghavan *et al.* (2005) used marine green alga *Ulva reticulata* and obtained a q_e of 55.6 mg/g. Tofan *et al.* (2013) observed a q_e of 12.49 mg/g using natural hemp fibers. Likewise, *Chrysanthemum indicum* was studied by Vilvanathan & Shanthakumar (2017a, 2017b), reporting a q_e of 9.32 mg/g at a flow of 5 mL/min and initial concentration of 50 mgL^{-1}. PM is in great advantage compared to these adsorbents; it is a raw material, derived from agricultural waste, which can be massively obtained from tea-based companies.

Likewise, k_{YN} and T^*k_{YN} represent the slope and y-intercept in the Yoon-Nelson linearized function, $ln(Ct/(C_0 - Ct)$ versus t graph. Rate constants of 0.107, 0.052 and 0.035 (L/min) values of k_{YN} were obtained for CM, GT and PM respectively (Table 1). Using the y-intercepts of the linearized Yoon-Nelson graphs (Figure 3), the values of t are determined using: $t = y\text{-intercept}/k_{YN}$. The values of t that represent the 50% adsorbate breakthrough times for CM, GT, and PM were determined to be 32.70, 53.99 and 109.44 (min) for CM, GT and PM respectively. These values indicate that PM has better pollutant retention, and a higher number of active sites that are able to hold more pollutant per mL of solution. GT could also be considered a good adsorbent due to its acceptable q_e from the Thomas' model and the t value from the Yoon-Nelson model. Our t values were compared to other pollutant/adsorbent systems from the literature. Li *et al.* (2018) adsorbed As (V) using a composite

Table 1 | Summary of results for the simulation of the adsorption of Co (II) on spent tealeaves

	Mathematical models											
	Thomas				Clark				Yoon-Nelson			
	k_{TH} (mL/min/mg)	q_e (mg/g)	R^2	RMSE	A(–)	r (min^{-1})	R^2	RMSE	k_{YN} (min^{-1})	t (min)	R^2	RMSE
CM	0.351	24.85	0.99	0.06	38.18	0.109	1.00	0.06	0.107	32.70	0.99	0.06
GT	0.191	25.20	0.97	0.15	27.12	0.060	0.97	0.15	0.052	53.99	0.97	0.15
PM	0.116	59.70	0.94	0.26	54.75	0.036	0.94	0.26	0.035	109.44	0.94	0.26

CM, GT and PM stand for chamomile, green and peppermint tealeaves respectively.

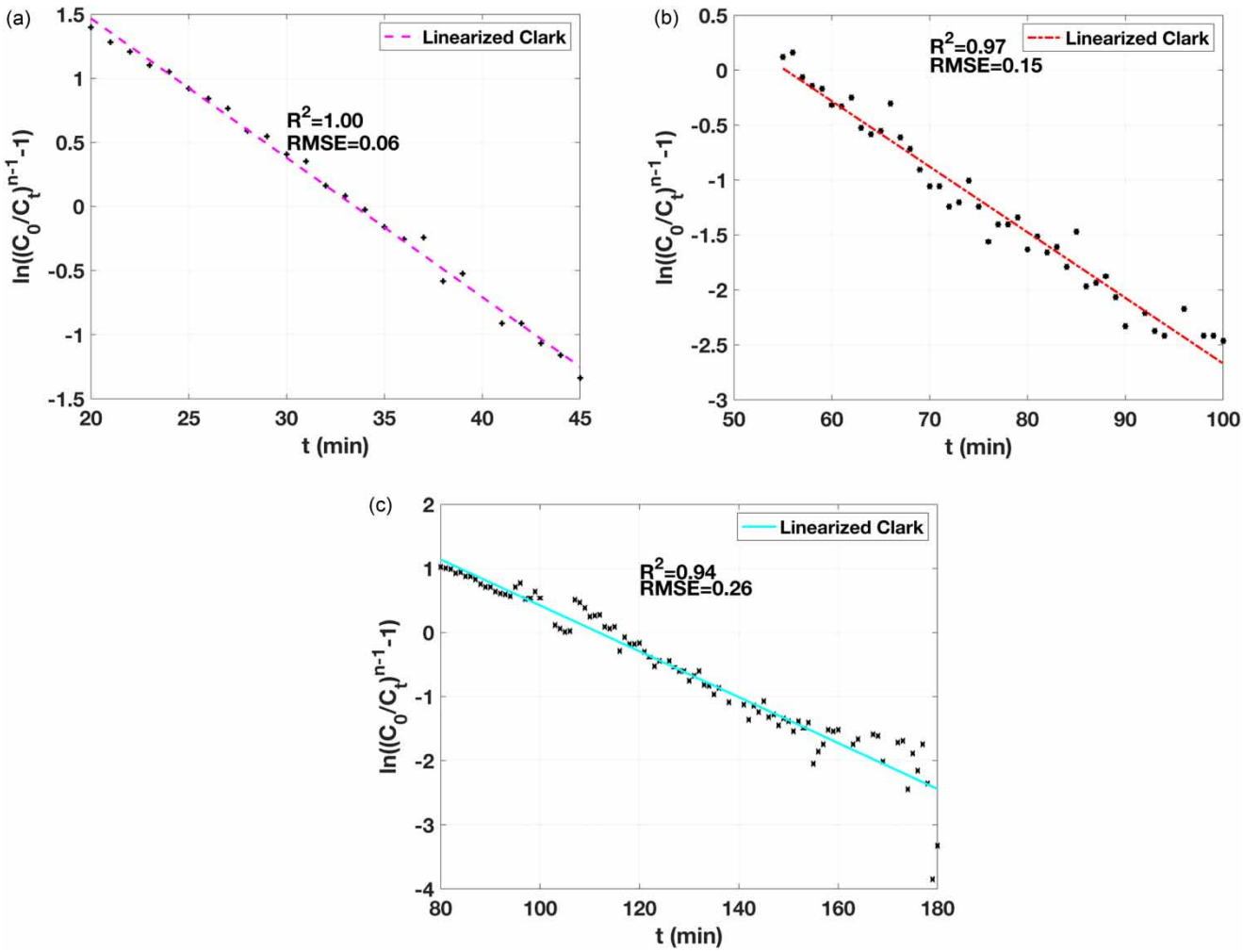

Figure 1 | Linearized Clark model for Co (II) ion adsorption on spent tealeaves. (a) For CM; (b) for GT; (c) for PM.

with eucalyptus wood, obtaining t values of 80 min, using the same mass of adsorbent in this experiment (~2 g).

Figures 1–3 also show the correlation coefficients and root-mean-squared-error (RMSE) values for the linearized models. The values are further summarized and depicted in Table 1. The correlations range from a minimum value of 0.94 for PM adsorbent to a maximum of 1.00 for the Clark model in the CM sample. The RMSE values between the experimental data and linearized model simulations were also calculated (shown in Table 1). All the simulation models from this study were able to simulate the contaminant effluent data very well. While the simulation of the experimental data in CM adsorbent is nearly perfect, with correlations of 0.99, 0.99 and 1.00 respectively, for Thomas, Yoon-Nelson and Clark models. There is a slight discrepancy between model output and experimental data in the PM adsorbent. All the three models also generated similar correlation and RMSE values for the respective adsorbent (Table 1). Using the Clark model, the best simulation of the adsorption data was obtained for CM tealeaves (correlation of 1.00 and RMSE = 0.06). The Thomas and Yoon-Nelson models generated correlations of 0.99, 0.97 and 0.94, and RMSE values of 0.06, 0.15, and 0.26 for CM, GT and PM, respectively.

The optimal parameters are substituted back to the model equations (Equations (1)–(3)) to simulate the adsorption breakthrough. Figures 4–6 show the experimental data as well as breakthrough graphs for the Clark, Thomas and Yoon-Nelson models, respectively. While the performances of these mathematical models were excellent in simulating the experimental data, it looks like they somehow failed to map the lower tails of the experimental data (Figures 4–6). Additional terms were added to the kinetic models to address the shortcomings of the models to delineate the lower part of the data.

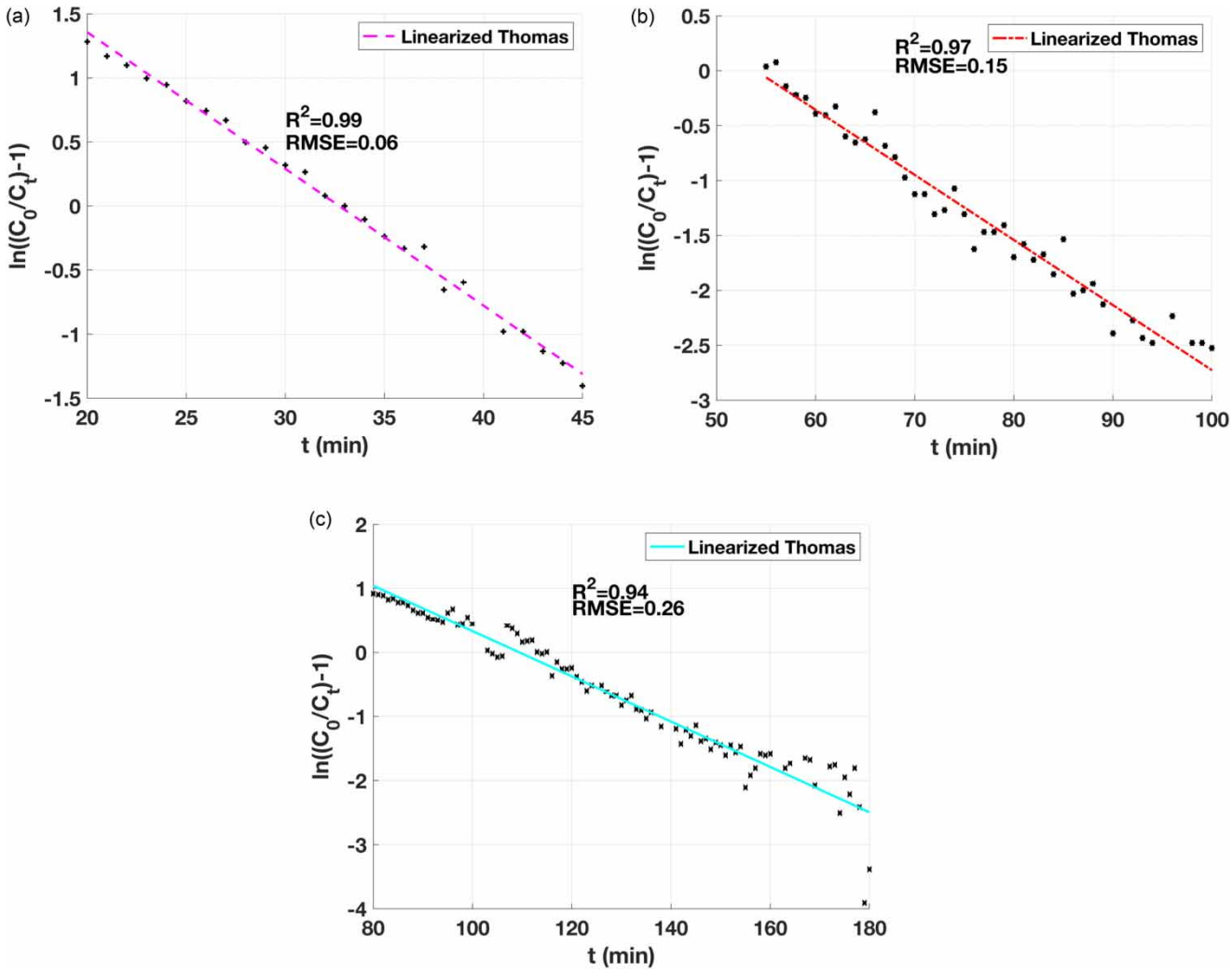

Figure 2 | Linearized Thomas model for Co (II) ion adsorption on spent tealeaves. (a) For CT; (b) for GT; (c) for PM.

Clark model with an additional term:

$$\frac{C_t}{C_0} = \left(\frac{1}{1+Ae^{-rt}}\right)^{\frac{1}{n-1}} + B_{Cl}\left[1 - \left(\frac{1}{1+Ae^{-\frac{t}{T_{Cl}}}}\right)^{\frac{1}{n-1}}\right] \quad (7)$$

Thomas model with an additional term:

$$\frac{C_t}{C_0} = \frac{1}{1+exp\left[\left(\frac{k_{TH}q_e x}{Q}\right) - k_{TH}C_0 t\right]} + B_{Th}\left[1 - \frac{1}{1+\exp\left[\left(\frac{k_{TH}q_e x}{Q}\right) - \frac{t}{T_{Th}}\right]}\right] \quad (8)$$

Yoon-Nelson model with an additional term:

$$\frac{C_t}{C_0 - C_t} = \exp(k_{yn}t - \tau k_{yn}) + B_{Yn}\left[1 - \frac{\exp\left(\frac{t}{T_{Yn}} - \tau k_{yn}\right)}{1+\exp\left(\frac{t}{T_{Yn}} - \tau k_{yn}\right)}\right] \quad (9)$$

where $B_{Cl,}$ B_{Th} *and* B_{Yn} are empirical constants for the Clark, Thomas and Yoon-Nelson models; $T_{Cl,}$ T_{Th} *and* T_{Yn} are the time constants for the Clark, Thomas and Yoon-Nelson models.

First, the data are modeled with the linearized functions (Equations (4)–(6)) to obtain the model parameters. After that, B and T are determined empirically (Table 2). Further study is required to determine the physical interpretation of the empirical parameters.

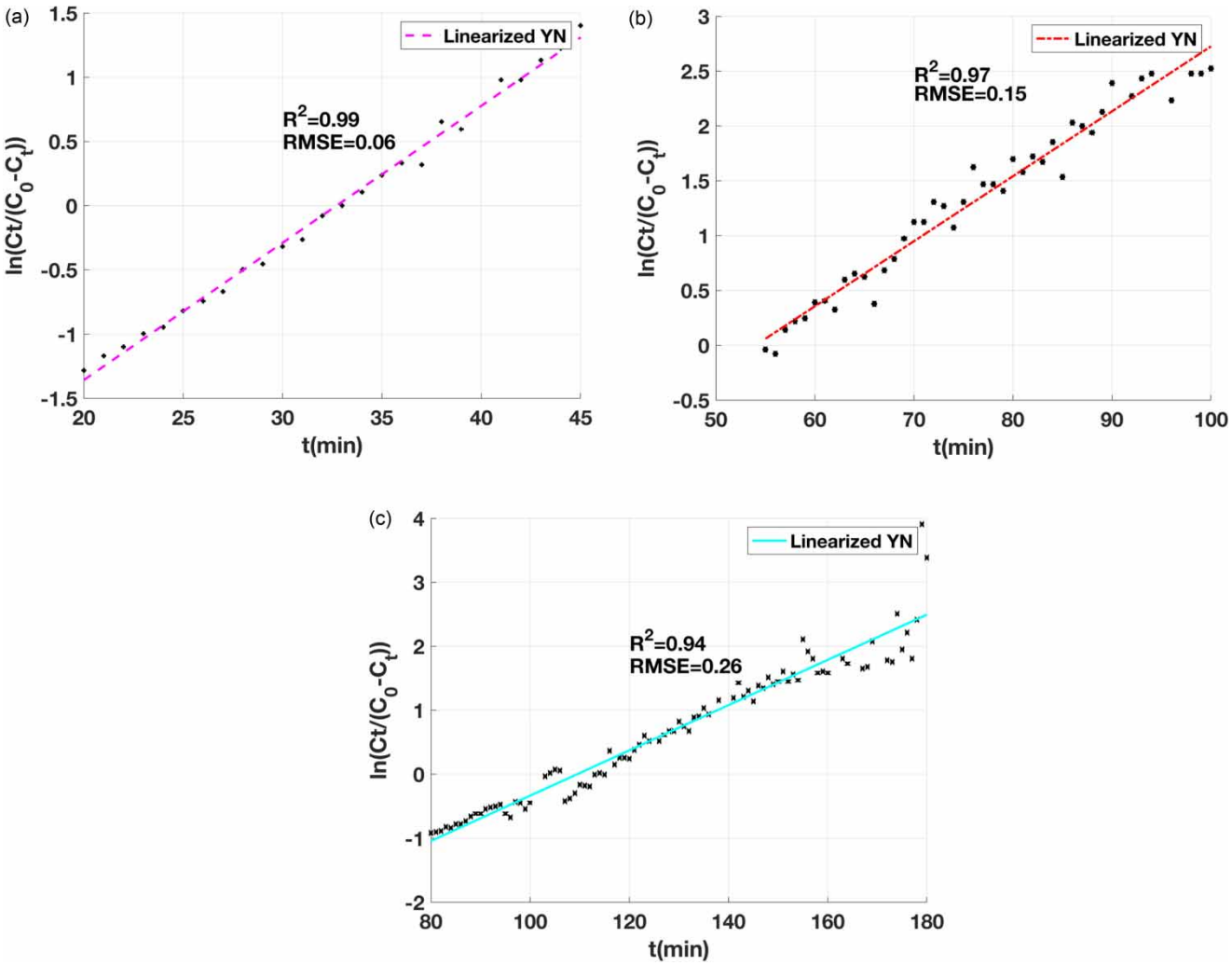

Figure 3 | Linearized Yoon-Nelson model for Co (II) ion adsorption on spent tealeaves. (a) For CM; (b) for GT; (c) for PM.

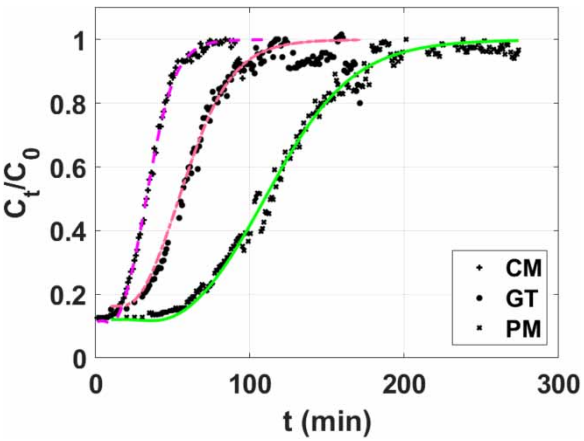

Figure 4 | Breakthrough curve for Co (II) ion adsorption on a fixed-bed column experiment using spent tealeaves. The symbols represent data points, the lines represent model simulations using the Clark model.

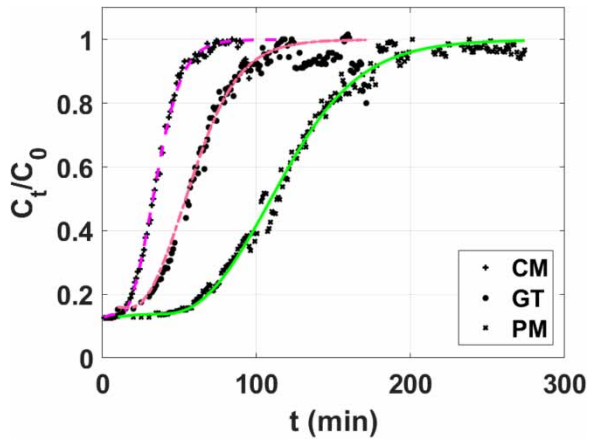

Figure 5 | Breakthrough curve for Co (II) ion adsorption on a fixed-bed column experiment using spent tealeaves. The symbols represent data points, the lines represent model simulations using the Yoon-Nelson model.

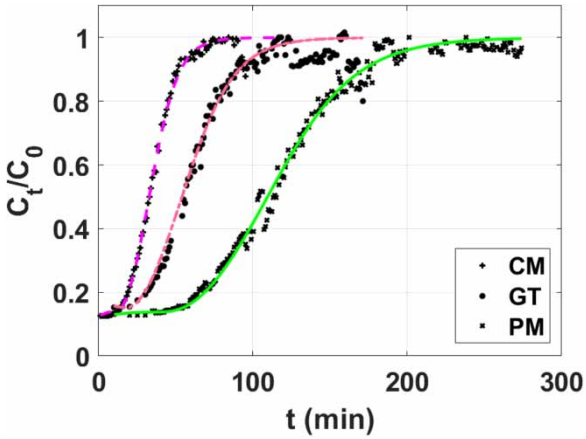

Figure 6 | Breakthrough curve for Co (II) ion adsorption on a fixed-bed column experiment using spent tealeaves. The symbols represent data points, the lines represent model simulations using the Thomas model.

Parameter sensitivity analysis

After determining the optimal parameter values for the models, a parameter sensitivity analysis was conducted for each mathematical adsorption model. This approach determines the influence of each parameter on the performance of the model. Negative and positive 15 (−15 and +15%) of the determined optimal values were calculated as the minimum and maximum values of the range of any of the parameters while keeping the remaining parameters at their optimal values. Then, the parameters range was divided into 20 equal parts. RMSE values between the model and experimental data are calculated for each value within the range while keeping the remaining parameters at their optimal values.

Figure 7 through 9 show the response of the RMSE to variation of each parameter around their optimal values. All the parameters that were investigated for sensitivity showed a common property: RMSE is equally sensitive to values less and larger than the optimal parameter values. Figure 8 displays the parameter sensitivity plot for Thomas' k_{TH} parameter. The rate at which the RMSE varies with k_{TH} is high, meaning that the model is sensitive to the variation of the model parameter.

Figure 7(a) and 7(b) show the parameter sensitivity plots for Clark's A and r model parameters. Figure 7(a) shows the change in RMSE gradient for the variation of parameter r is higher than that of parameter A. Hence, the Clark model is more sensitive to the variation of r than A.

Similarly, the two parameters k_{YN} and t in the Yoon-Nelson model were plotted against RMSE between experimental data and model output (Figure 9(a) and 9(b)). The sensitivity of RMSE to the rate constant (k_{YN}) and the time required for 50% adsorbate breakthrough (t) in Yoon-Nelson's model is shown in Figure 9.

Morphological and textural characterization of the adsorbents

The scanning electron micrographs of the three adsorbents are shown in Figure 10. From the images, it can be concluded that the surface of PM is more heterogeneous, where pores, cavities, hills, pockets and veins blend on the relief of the adsorbent. The presence of the features is more obvious at ×1200 zoom, where it can be confirmed that Co (II) and any pollutant will be easily trapped or can potentially get lost inside the roughness of PM. Conversely, CM displays a more homogeneous surface, where hills and veins are still observed but the surface is not as saturated by these imperfections as in PM. At higher zoom, CM appears more homogeneous, only showing isolated pores and big valleys. It is important to highlight that even though the three adsorbents were purchased as teabags,

Table 2 | Summary of empirical constants for the kinetics models for the simulation of the adsorption of Co (II) on spent tealeaves

	Additional empirical parameters					
	Thomas		Clark		Yoon-Nelson	
	$B_{Th,}$	T_{Th}	B_{Cl}	T_{Cl}	B_{YN}	T_{YN}
CM	0.09833	3.2172	0.08409	11.729	0.09855	3.0413
GT	0.1152	4.9362	0.11302	26.841	0.1152	5.2901
PM	0.1068	10.891	0.09935	52.559	0.10601	11.11

CM, GT and PM stand for chamomile, green and peppermint tealeaves respectively.

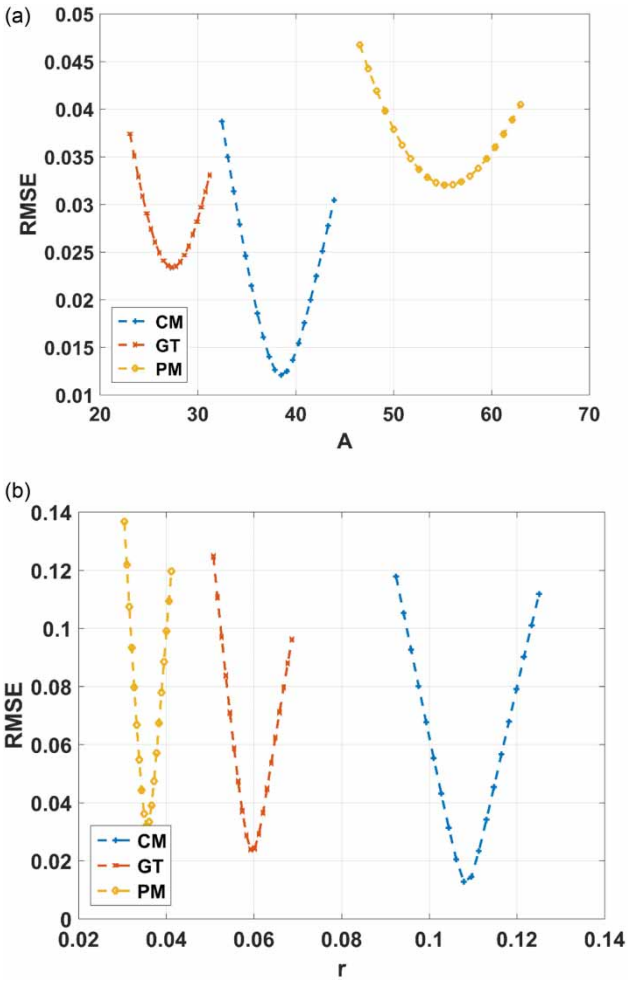

Figure 7 | Parameter sensitivity analysis for Clark's model parameters (A and r) for the adsorption of Co (II) ions on chamomile (CM), green (GT) and peppermint (PM) tealeaves.

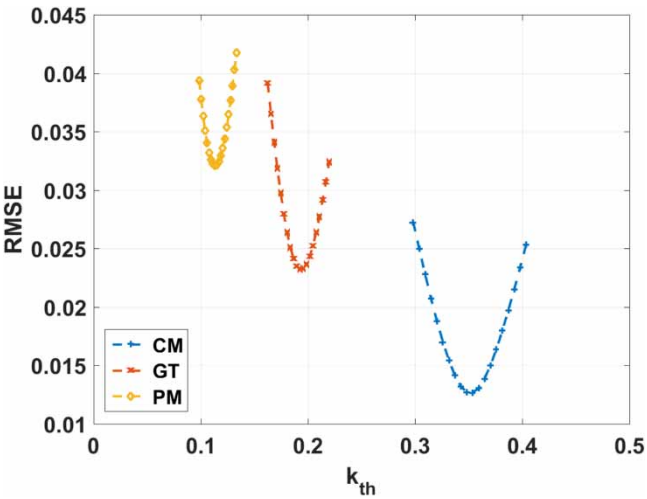

Figure 8 | Parameter sensitivity analysis for Thomas' model parameter (k_{th}) for the adsorption of Co (II) ions on chamomile (CM), green (GT) and peppermint (PM) tealeaves.

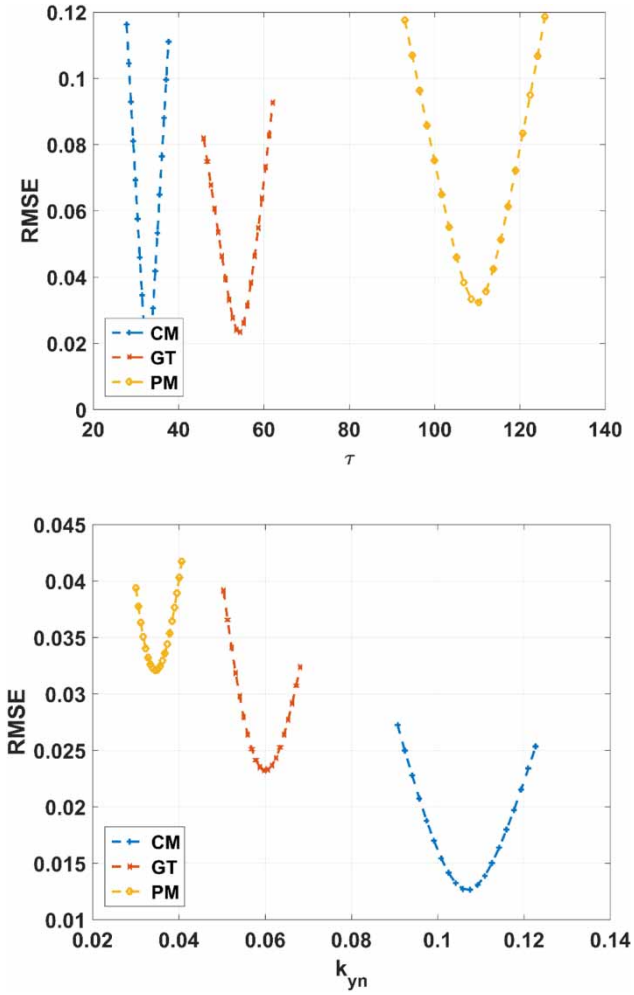

Figure 9 | Parameter sensitivity analysis for Yoon-Nelson's model parameters (t and k_{yn}) for for the adsorption of Co (II) ions on chamomile (CM), green (GT) and peppermint (PM) tealeaves.

CM is really a flower and not a leaf like GT and PM. Therefore, CM is expected to have a softer surface due to its physiological role in the plant life. On the other hand, GT displays an intermediate morphology and texture, with a combination of big pores, veins, pockets and protrusions on the surface. GT's surface looks closely like the surface of PM. Therefore, it could be hypothesized that the difference in adsorption capacity (Thomas's q_e) does not reside on the morphological surface differences of the GT and PM adsorbents, but on the presence and concentration of active functional groups. In their most recent book, Crini & Lichtfouse (2018) indicated that lignocellulosic materials like spent tealeaves contain polar functional groups such as carboxyl, hydroxyl, amino, thiol, sulfonic, imine, and hemiacetal amongst others, and their

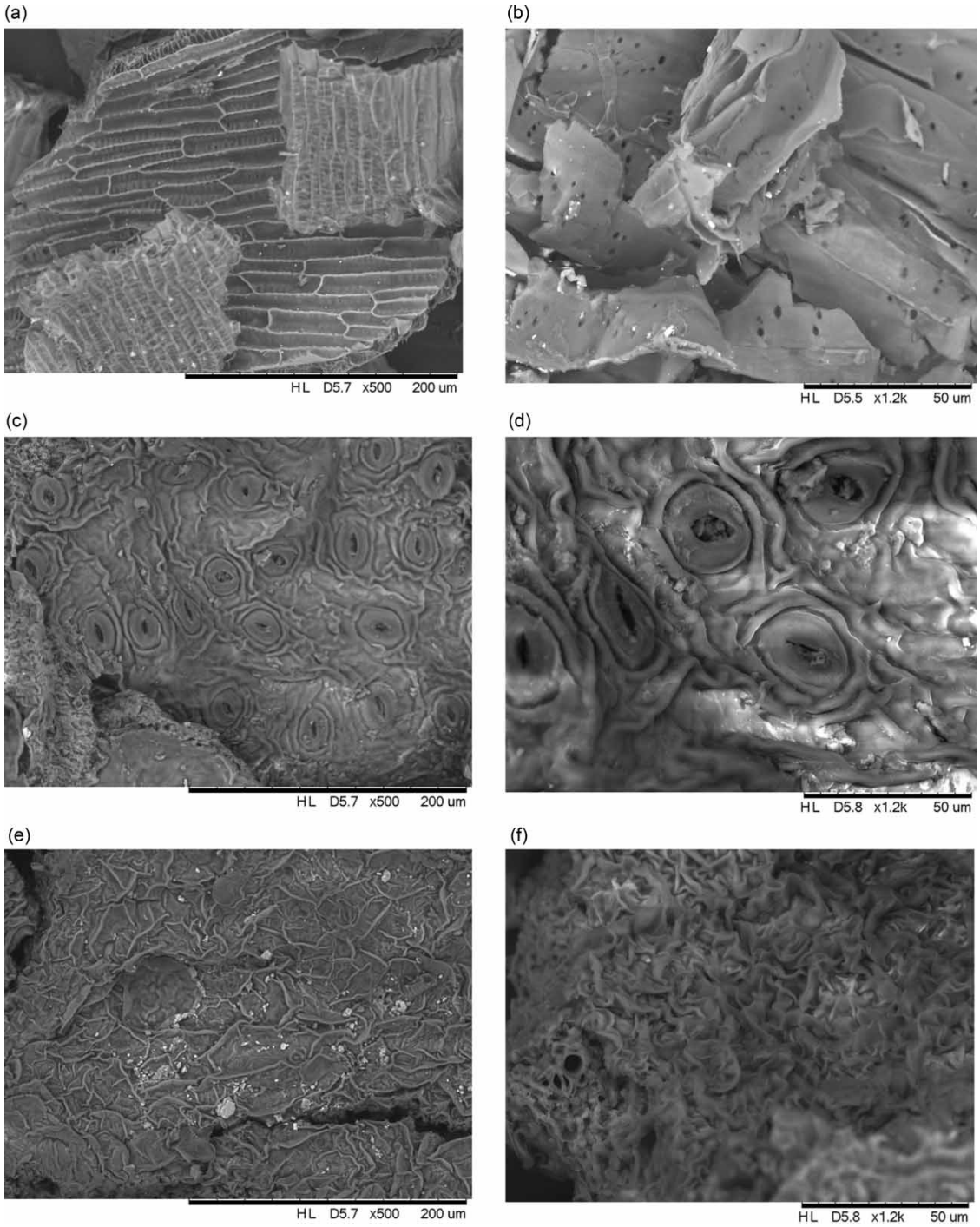

Figure 10 | Scanning electron micrographs of CM (a and b), GT (c and d) and PM (e and f) at two different magnifications.

concentration varies from species to species. Therefore, since the morphology of GT and PM are very similar, it could be concluded that PM has more functional groups in diversity or quantity that make it more efficient on the removal of Co (II) ions from solutions. This is reflected on the PM Thomas's q_e value (more than two-fold compared to GT) and the 50% breakthrough time value (t) according to Yoon-Nelson's theory. Further studies like a meticulous infrared spectroscopy, elemental analysis by energy dispersion with X-ray spectroscopy are needed

to evidence the types and quantities of these active adsorption sites.

CONCLUSIONS

The experimental results showed that spent tealeaves and chamomile have promising ability to remove heavy metals from aqueous solutions. Adsorption dynamics assays indicated that the breakthrough equations fit the experimental data accurately according to the theories of Clark, Thomas and Yoon-Nelson. The model simulation outcomes were very similar, only varying by a small margin. The linearization of the models helped accurately determine the model parameters. The results indicated that PM was a better adsorbent when compared to GT and CM. According to Thomas' model, equilibrium adsorption capacity values for PM, GT, and CM were 59.7, 25.2, and 24.9 mg/g, respectively. On the other hand, Yoon-Nelson modeling indicated 50% breakthrough time values of 109, 54, and 33 min for PM, GT and CM, respectively. Parameters sensitivity analysis showed that the Clark model was more sensitive to changes in A than r. In the Yoon-Nelson model, variation in t had more influence on the model than K_{YN}. Scanning microscopy tests displayed optimum adsorbent morphology and textural properties for all three adsorbents; however, a more heterogeneous surface was observed in PM and GT, showing pores, veins, hills, and pockets as the main component of their surfaces. The next step is to carry out parameter sensitivity analysis as well as changing the independent variables including flow rate, influent concentration, and bed height. This will prove if the adsorption of heavy metals using spent tealeaves is dependent on different controlled variables of the experiment. The performance analysis of the breakthrough curve can be defined well by the Thomas, Clark, and Yoon-Nelson models. Lastly, further insights into the mechanism of adsorption can be elucidated with infrared and X-ray spectroscopies to investigate the functional groups that are responsible for the uptake of Co (II) ions from solutions.

ACKNOWLEDGEMENTS

This study was supported by CUNY's Community College Collaborative Incentive Research Grant (C^3IRG). A.N. thanks the financial support of PSC-CUNY grant and BMCC Faculty Publication Grant.

REFERENCES

Ahluwalia, S. S. & Goyal, D. 2005 Removal of heavy metals by waste tea leaves from aqueous solution. *Engineering in Life Science* **5** (2), 158–162.

Crini, G. & Lichtfouse, E. (eds) 2018 Green adsorbents for pollutant removal – innovative materials. Environmental chemistry for a sustainable world. Springer Nature Switzerland, Dordrecht, The Netherlands, p. 399.

Jung, S., Naidoo, M., Shairzai, S. & Navarro, A. E. 2014 On the adsorption of a cationic artificial dye on spent tea leaves. *WIT Transactions on The Built Environment* **139**, 231–241.

Kim, T., Yang, D., Kim, J., Musaev, H. & Navarro, A. 2013 Comparative adsorption of highly porous and raw adsorbents for the elimination of copper (II) ions from wastewaters. *Trends in Chromatography* **8**, 97–108.

Li, Y., Zhu, Y., Zhu, Z., Zhang, X., Wang, D. & Xie, L. 2018 Fixed-bed column adsorption of arsenic (V) by porous composite of magnetite/hematite/carbon with eucalyptus wood microstructure. *Journal of Environmental Engineering and Landscape Management* **26** (1), 38–56.

Mahvi, A. H., Naghipour, D., Vaezi, F. & Nazmara, S. 2005 Teawaste as an adsorbent for heavy metal removal from industrial wastewaters. *American Journal of Applied Sciences* **2** (1), 372–375.

Malakahmad, A., Tan, S. & Yavari, S. 2016 Valorization of wasted black tea as a low-cost adsorbent for nickel and zinc removal from aqueous solution. *Journal of Chemistry* **2016**, 1–8.

Massimi, K., Giuliano, A., Astolfi, M. L., Congedo, R., Masotti, A. & Canepari, S. 2018 Efficiency evaluation of food waste materials for the removal of metals and metalloids from complex multi-element solutions. *Materials* **11**, 334.

Patel, H. 2019 Fixed-bed column adsorption study: a comprehensive review. *Applied Water Science* **9** (3), 45.

Rengaraj, S. & Moon, S. H. 2002 Kinetics of adsorption of Co (II) removal from water and wastewater by ion exchange resins. *Water Research* **36** (7), 1783–1793.

Saadi, Z., Saadi, R. & Fazaeli, R. 2013 Fixed-bed adsorption dynamics of Pb (II) adsorption from aqueous solution using nanostructured γ-alumina. *Journal of Nanostructure in Chemistry* **3** (1), 48.

Sotelo, J. L., Ovejero, G., Rodríguez, A., Álvarez, S. & García, J. 2013 Adsorption of carbamazepine in fixed bed columns: experimental and modeling studies. *Separation Science and Technology* **48** (17), 2626–2637.

Tofan, L., Teodosiu, C., Paduraru, C. & Wenkert, R. 2013 Cobalt (II) removal from aqueous solutions by natural hemp fibers: batch and fixed-bed column studies. *Applied Surface Science* **285**, 33–39.

Vijayaraghavan, K., Jegan, J., Palanivelu, K. & Velan, M. 2005 Biosorption of copper, cobalt and nickel by marine green alga *Ulva reticulata* in a packed column. *Chemosphere* **60** (3), 419–426.

Vilvanathan, S. & Shanthakumar, S. 2017a Column adsorption studies on nickel and cobalt removal from aqueous solution using native and biochar form of *Tectona grandis*. *Environmental Progress & Sustainable Energy* **36** (4), 1030–1038.

Vilvanathan, S. & Shanthakumar, S. 2017b Modeling of fixed-bed column studies for removal of cobalt ions from aqueous solution using *Chrysanthemum indicum*. *Research on Chemical Intermediates* **43** (1), 229–243.

Xavier, A. L. P., Adarme, O. F. H., Furtado, L. M., Ferreira, G. M. D., da Silva, L. H. M., Gil, L. F. & Gurgel, L. V. A. 2018 Modeling adsorption of copper (II), cobalt (II) and nickel (II) metal ions from aqueous solution onto a new carboxylated sugarcane bagasse. Part II: optimization of monocomponent fixed-bed column adsorption. *Journal of Colloid and Interface Science* **516**, 431–445.

Yang, X. & Cui, X. 2013 Adsorption characteristics of Pb (II) on alkali treated tea residue. *Water Resources and Industry* **3**, 1–10.

Zuorro, A. & Lavecchia, R. 2010 Adsorption of Pb(II) on spent leaves of green and black tea. *American Journal of Applied Sciences* **7** (2), 153–159.

First received 18 February 2020; accepted in revised form 7 June 2020. Available online 18 June 2020